UCRL-CONF-213044

LAWRENCE
LIVERMORE
NATIONAL
LABORATORY

High-resolution ab-initio three-dimensional coherence X-ray diffraction microscopy

A. Barty, H.Chapman, S. Marchesini, M. Howells, C. Jacobsen, J. Kirz, J. Spence, C. Cui, U. Weierstall, H. He

June 20, 2005

Coherence 2005
Porquerolles, France
June 14, 2005 through June 18, 2005

High-resolution *ab initio* three-dimensional coherent X-ray diffraction imaging

A. Barty[1], H. N. Chapman[1], S. Marchesini[1], M. R. Howells[2], C.Jacobsen[3], J.Kirz[2,3], J. C. H. Spence[2,4], T. Beetz[3], C. Cui[2], U. Weierstall[4], H. He[2]

[1] Lawrence Livermore National Laboratory, 7000 East Avenue, Livermore, CA, 94550-9234, USA
[2] Lawrence Berkeley National Laboratory, 1 Cyclotron Rd, Berkeley, CA, 94720, USA
[3] Department of Physics, State University of New York, Stony Brook, NY 11794, USA
[4] Arizona State University, Department of Physics, Tempe, Arizona, 85287-1504, USA

Overview

Three-dimensional diffraction microscopy offers the potential for high-resolution aberration-free diffraction-limited 3D images without the resolution and depth-of-field limitations of lens-based tomographic systems.

Critical issues in obtaining a high-quality image include:
- Data collection: signal to noise, system stability, dynamic range, automation
- Alignment of diffraction patterns with respect to one another
- Assembly of the diffraction data into a diffraction volume
- Efficient algorithms for applying phase retrieval techniques to the diffraction volume
- Stability of the three-dimensional phase retrieval process
- Techniques for determining the object support; and
- Treatment of missing data, both within the beamstop region and elsewhere.

We have obtained high-quality 3D reconstructions from X-ray diffraction data alone. This is an important step, as it does not require a low-resolution image to fill in the beamstop region.

Data collection

- Data collected at beamline 9.0.1 at the Advanced Light Source (ALS), Berkeley using an end-station built by Chris Jacobsen's team at State University of New York at Stony Brook.
- The beamline delivers a coherent flux of 8×10^9 photons/sec into a 4μm pinhole with $\Delta\lambda/\lambda$ of several thousand using an off-axis zone plate / pinhole pair monochromator.
- Sample positioning uses a motorised four-axis goniometer system provided by JEOL USA, Inc., which is normally a component of their JEM-2010 FasTEM transmission electron microscope.
- In-vacuum CCD camera from Roper Scientific has a backside-illuminated 1340x1300 pixel CCD with 20μm pixels and a claimed readout noise of 4 electrons RMS per pixel.
- Dynamic range of the CCD is limited to 200000 electrons full well capacity, so several exposures ranging from 0.5sec to 100sec are merged in software to produce a single image with dynamic range several times that of the CCD chip itself.

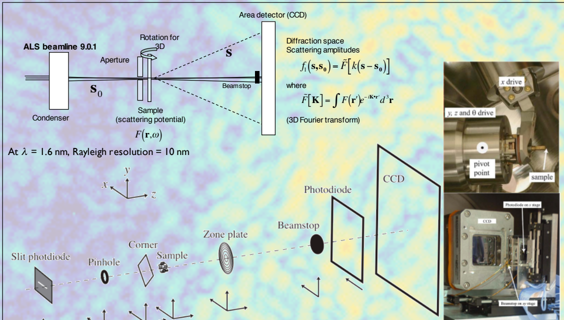

See T..Beetz *et.al.* Nuclear Instruments and Methods, 2005.

Data assembly and preprocessing

The measured 2D diffraction patterns must first be converted into a 3D data cube:

- Assembly of the 3D diffraction volume is performed by mapping the 2D (x,y) co-ordinates of each pixel in the measured diffraction pattern onto the Ewald sphere using the known distance from sample to detector, beam energy and CCD pixel size and to determine the Ewald sphere curvature.
- A 3D rotation matrix from the known sample orientation is then applied to these coordinates to determine the 3D coordinates of each measured pixel in the diffraction volume.
- The rotated Ewald sphere diffraction patterns are mapped onto a regular 3D cartesian voxel grid using nearest-neighbour sampling.
- Where more than one pixel from the set of intensity measurements contributed to a given voxel, the pixel values are averaged to determine the appropriate intensity value at that point.
- Only the measured diffraction data are used – no other sample information or measurements were used in reconstruction process.
- No low-resolution measurements are used to fill in the beamstop region and no numerical interpolation is performed between the measured Ewald spheres.
- For the case of the pyramid data set (shown below) 149 diffraction patterns were measured spanning sample angles from -45 to +78 degrees sample rotation.

IDL tool used to process measured 2D images into a 3D diffraction volume

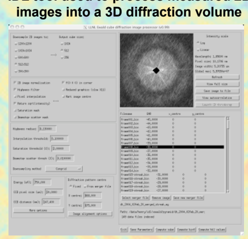

3D view of a diffraction volume

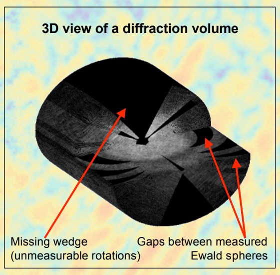

Orthogonal slices through the diffraction volume

K_y=0 slice K_z=0 slice K_x=0 slice

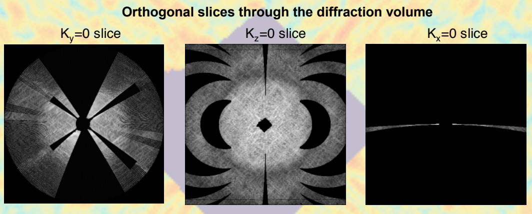

Computational reconstruction

Each reconstruction requires at least the following:

- Two complex arrays (reconstructions)
- One floating point array (input data)
- One byte mask (support)
- 1000 or more 3D FFTs

Memory and calculation requirements are significant and suggest a cluster-based solution.

Memory requirements[1]		
Size	Single precision	Double precision
256^3	336MB	592MB
512^3	2.6GB	4.7Gb
1024^3	22GB	38GB
2048^3	176GB	304GB

We use the *dist_fft* distributed fast Fourier transform library from Apple Computer for optimum Fourier transformn speed. *dist_fft* has been hand-optimised for the G5 vector processor architecture by the Apple Advanced Computation Group and uses standard MPI interfaces to perform distributed giga-element or larger FFTs.

Reconstruction code is written in C, is fully parallelised, and uses distributed memory and MPI interfaces to share the workload across all CPUs in the system. This includes application of real and Fourier space constraints and dynamic support refinement using the *Shrinkwap* algorithm.

We use a 16-node 2.0GHz dual processor (32 processors total) Xserve G5 cluster with low latency Infiniband interconnects and 4GB RAM per node.

Reconstructions presented here were performed on a 512^3 grid enabling us to produce a high-quality reconstruction in 1.5 to 2 hours.

Reconstruction speed on 16-node, 32-CPU 2.0GHz Xserve G5 cluster		
Size	Per 3D FFT	Full reconstruction[2]
256^3	73msec	10 mins
512^3	850msec	1.5 hrs
1024^3	7.9sec	14 hrs

[1] Assumes minimum of 2x complex data cubes for FFTs, 1x diffraction data cube (real), 1x support array (byte)
[2] Based on 2000 iterations, 2FFTs per iteration plus other floating point operations needed for the reconstruction

Diffraction-space constraints Real-space constraints

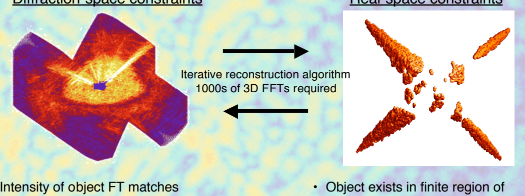

Diffraction-space constraints:
- Intensity of object FT matches measured diffraction intensity
- Missing data allowed to float
- *No low-resolution data to fill in beamstop region*

Real-space constraints:
- Object exists in finite region of space (finite support)
- Object is real-valued (optional)
- Object is positive definite (optional)

3D images from experimental data

- Test object consists of a microfabricated silicon nitride pyramid decorated with 50nm gold balls, as shown in the SEM images below.
- 149 diffraction patterns were measured spanning sample angles from -45 to +78 degrees in steps of 0.5 to 1.0 degrees at an X-ray energy of 750eV.
- Individual diffraction images are arranged into a 3D diffraction cube using known sample rotation angles. The assembled 3D diffraction volume has been shown above.

SEM image of microfabricated pyramid test object

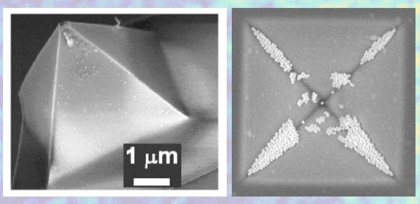

Silicon Nitride pyramid decorated with 50nm gold balls

- Reconstruction performed on a 512^3 grid using MPI code on our G5 cluster.
- Initial support estimate is generated by extruding a 2D reconstruction into 3D, and can also be generated from autocorrelation of diffraction data.
- Subsequent support refinement using *Shrinkwrap* every 30 iterations.
  Support threshold of 15%, initial convolution radius of 1.2 pixels Gaussian FWHM, reducing to 0.75 pixels in steps of 2% per application.
- HIO algorithm used for first 600 iterations, then RASR algorithm to iteration 2500.
- Object allowed to be complex valued - no reality or positivity constraint applied at this stage.

3D image reconstructed from X-ray diffraction data alone
(isosurface rendering)

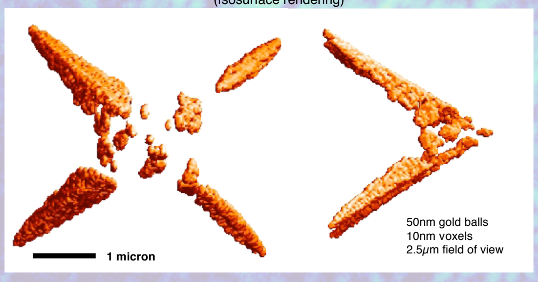

Orthogonal slices through reconstructed diffraction volume

K_y=0 slice K_z=0 slice K_x=0 slice

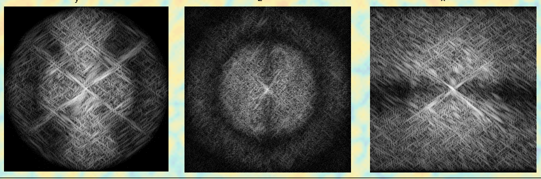

- Missing data (including the beamstop region) are allowed to float.
- Regions of missing data are filled in by the reconstruction code, producing a continuous diffraction pattern representing the object.

Application of material constraints

For X-rays, the reconstructed scattering potential takes the form:

$$F(\mathbf{r},\omega) = \frac{1}{4\pi}k^2\left[n^2(\mathbf{r},\omega) - 1\right]$$

$$n = 1 - \delta - i\beta$$

$$\boxed{F(\mathbf{r},\omega) = \frac{1}{2\pi}k^2\left[-\delta - i\beta + O(\delta,\beta)^2\right]}$$

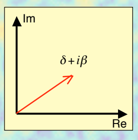

- For a single material the ratio of δ and β is constant, thus all voxels should have the same relative phase. Voxel values should line on a line in the complex plane.
- For multiple material objects the range of allowed δ and β values will lie within a wedge composed of the linear sum of all δ,β values for all materials in the object.
- Application of the single material phase constraint to our gold ball pyramid data produced the following result:

Orthogonal maximum intensity projections with constant phase constraint applied

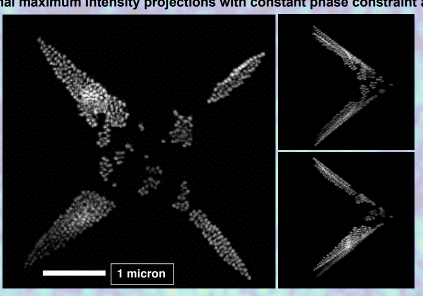

3D imaging of low density foams

We have applied 3D diffraction imaging to determining the 3D structure of low density aerogel foam samples. These foams are low density (100mg/cc) and have an internal skeleton structure composed of Ta_2O_5.

Data collection and processing is similar to that used for the pyramid object. For ease of handling the sample was placed on a silicon nitride membrane which collected some debris (as shown in reconstruction to the left).

Scientific question is: How isotropic and uniform are these foams, and how does processing alter their structure?

3D structure measured using diffraction imaging is being used to answer this question.

3D reconstruction of foam sample

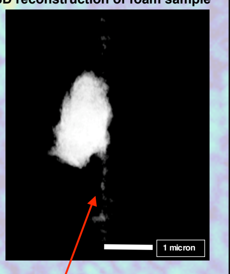

Debris particles on membrane

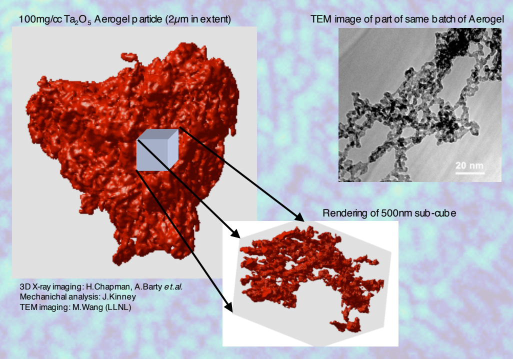

Key references:
- R. Crandall *et.al.* "Gigaelement FFTs on Apple G5 clusters" (2004) http://www.apple.com/acg, http://images.apple.com/acg/pdf/20040827_GigaFFT.pdf
- S. Marchesini *et.al.* "X-ray image reconstruction from a diffraction pattern alone" Phys Rev B 68, 140101R 2003.
- T..Beetz *et.al.* "Apparatus for X-ray diffraction microscopy and tomography of cryo specimens" Nuclear Instruments and Methods, 2005 (in press).

This work was performed under the auspices of the US Department of Energy by University of California Lawrence Livermore National Laboratory under contract No. W-7405-Eng-48 and Lawrence Berkeley National Laboratory.

Background: Measured diffraction pattern from pyramid test object (logarithmic intensity scale)

14 June 2005